Title	Melting of Aluminum Alloy by Using Gas Tunnel Type Plasma Jet(Physics, Process, Instruments & Measurements)
Author(s)	Kobayashi, Akira; Zhang, Jinqiu
Citation	Transactions of JWRI. 1992, 21(1), p. 17-22
Version Type	VoR
URL	https://doi.org/10.18910/7146
rights	
Note	

Melting of Aluminum Alloy by Using Gas Tunnel Type Plasma Jet[†]

Akira KOBAYASHI* and Jinqiu ZHANG**

Abstract

By using a gas tunnel type plasma jet, the melting of aluminum alloy was carried out. In this plasma system high thermal efficiency could be obtained: the efficiency of this plasma jet was about 70%. The transferred energy from the plasma jet was large at a short operating distance.

In this paper, the fundamental characteristics of this melting system were studied by changing the experimental conditions such as the distance from plasma torch, the power input to the torch. The melting time was increased as the melting distance was increased, which caused the decrease of the melting efficiency. This melting system had a higher melting efficiency when the power input (to plasma torch) was large at a short melting distance.

Furthermore, in order to investigate the property of melted aluminum alloy the thermal effect of plasma melting on the Vickers hardness of the specimen and the composition of the melted specimen were discussed. The hardness of this melting alloy became lower than that of as received aluminum alloy as well as the case of heat treatment.

KEY WORDS: (Gas Tunnel Type Plasma Jet), (Thermal Effciency), (Plasma Melting), (Aluminum Alloy), (Transferred Energy), (Melting Distance), (Melting Efficiency), (Vickers Hardness)

1. Introduction

Gas tunnel type plasma jet is an excellent heat source which is very stable and has a high temperature and a high energy density[1,2]. The length of its falme is longer, and the thermal efficiency is much higher than that of the conventional type of plasma jet[3].

Therefore, this plasma system makes it easy to apply to such fields as thermal processing of various materials which includes welding, cutting, coating, melting and refining and so on[4].

For example, the detailes of the application of the gas tunnel type plasma jet to plasma spraying have been previously reported[5,6,7].

Namely, the characteristics of ceramic sprayed coatings which were formed by the gas tunnel type plasma spraying were investigated. The relations between the spraying conditions and the Vickers hardness on the cross sections of ceramic sprayed coatings were clarified[6,7].

In alumina and zirconia coating by using the gas tunnel type plasma spraying, the Vickers hardness of the coating was increased with decreasing spraying distance, and a higher Vickers hardness could be obtained in the case of a shorter spraying distance[8,9].

In this paper, for the purpose of applying this plasma system to melting of metals, the melting of aluminum alloy by using the gas tunnel type plasma jet was investigated in detail: the influence of the experimental conditions — power input to plasma torch and distance from the torch (melting distance) — on the thermal efficiency of this torch and melting efficiency of the aluminum alloy was measured. The fundamental characteristics of this plasma melting system were clarified, and the property of the melted aluminum alloy was discussed by using a microscope and a microhardness tester.

2. Experimentals

The gas tunnel type plasma jet apparatus used in this study is shown in **Fig. 1(a)**. In this case, the gas divertor nozzle which is the exit electrode nozzle had a diameter of $d = 13.5$mm. The experimental methods to operate the gas tunnel type plasma jet have been described in the previous papers[1,2,5].

The working gas for this gas tunnel type plasma torch was argon (Ar). The gas flow rate was $Q = 2001/\text{min}$, which was a half value as compared with the former ones[1,2]

(a) Gas tunnel type plasma jet,   (b) Specimen and melting pot.
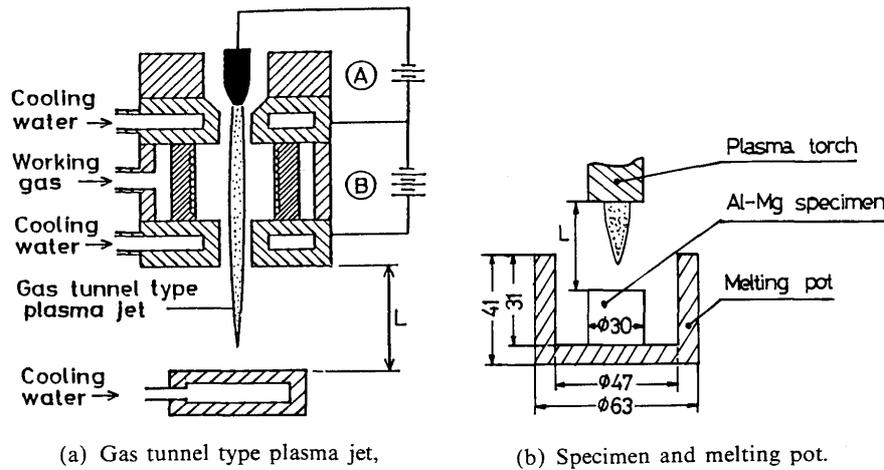
Fig. 1 Gas tunnel type plasma jet apparatus.

Table 1 Chemical composition of aluminum alloy used.

Material	Al	Fe	Si	Cu	Mn	Mg	Cr	Zn	Ni
wt%	94.8	0.11	0.02	0.01	0.07	4.9	0.05	0.01	0.01

At first, the thermal efficiency of this type of plasma torch was obtained by the calorimetric method through the measurement of temperature of the cooling water for the torch.

The transferred energy from the plasma jet to the substrate was also measured calorimetrically by using the water cooled copper plate which is shown in Fig. 1(a). The substrate was fixed at each distance from the plasma torch (operating distance) and the heat transfer from the plasma was measured.

The experiment for the plasma melting of aluminum alloy by using this gas tunnerl type plasma was carried out under the following conditions. The power input to the plasma torch was from $P=15$kW, to $P=25$kW, and the distance from torch (melting distance) was from $L=30$mm to $L=50$mm. Ar gas flow rate for gas tunnel type plasma spraying torch was $Q=200$l/min.

As melting material, we used Al-Mg alloy in this study. Table 1 shows the chemical composition of this aluminum alloy used. This was commercially prepared rod type of Al5056. And the size of the specimen of aluminum alloy was 30mm in diameter, and 25mm in length. The profile of the melting pot and the specimen are shown in Fig. 1(b). Here, L shows the melting distance: distance between the specimen and the plasma torch. The specimen was fixed to melt at each melting distance L.
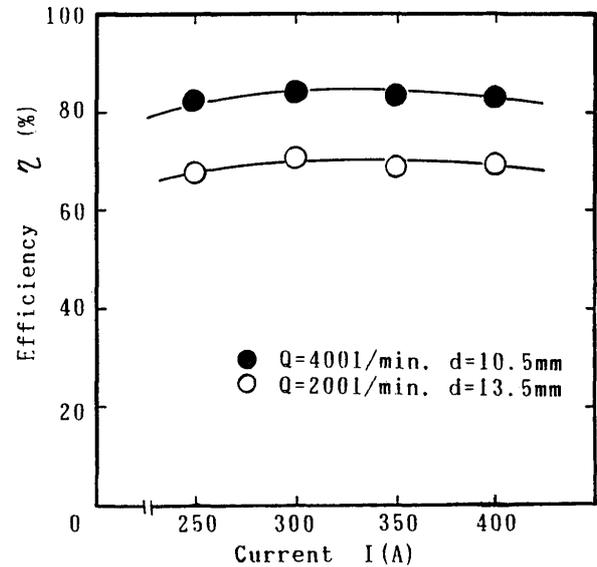

Fig. 2 Thermal efficiency of gas tunnel type plasma jet.

For the melted aluminum alloy, the chemical composition was measured by the atomic absorption spectrocheminical analysis.

The measurement of the Vickers hardness of the aluminum alloy was carried out in the cross section of the specimen, under the condition that the load weight was 100g and its load time was 25s.
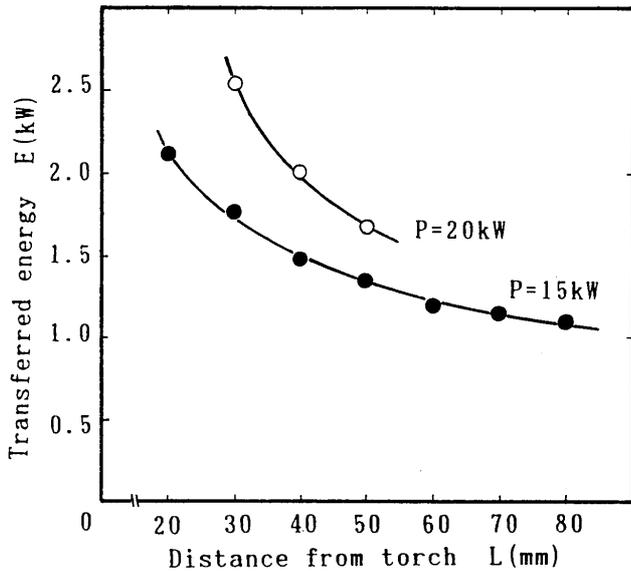
Fig. 3 Dependence of transferred energy on distance from torch (operating distance) at $P=15$kW and $P=20$kW.

Fig. 4 Dependence of melting percentages of aluminum on operating time at $L=30$mm, 40mm and 50mm, when $P=20$kW.

In comparison with the plasma melting, a heat treatment was carried out in air in an electric furnace at various temperatures for 30 minutes. After heat treatment the specimen was naturally cooled in air.

3. Results and Discussion

3.1 Thermal efficiency of gas tunnel type plasma jet

Figure 2 shows the thermal efficincy of gas tunnel type plasma jet, which was obtained by the calorimetric measurement.

In this case, the experiment was carried out under the following condition: the gas divertor nozzle had a diameter of $d=13.5$mm, the arc current was changed from 250A to 400A, which corresponded to the power input of $P=12-25$kW. Ar gas flow rate was $Q=200$l/min.

The results obtained in this study are indicated by the data of white circles in this figure. From these results, it is found that the thermal efficiency of gas tunnel type plasma jet was very high value of about $\eta=70\%$. Because many types of conventional plasma jet have the thermal efficiency of $50-60\%$.

While, for the comparison, the thermal efficiency of gas tunnel type plasma jet obtained by the former study was indicated by black circles in the same figure. In this study, the value of thermal efficiency was lower value than that of the former one: $\eta=80\%$. This reason is thought that the gas flow rate was smaller than the former case.

3.2 Heat transfer of gas tunnel type plasma jet

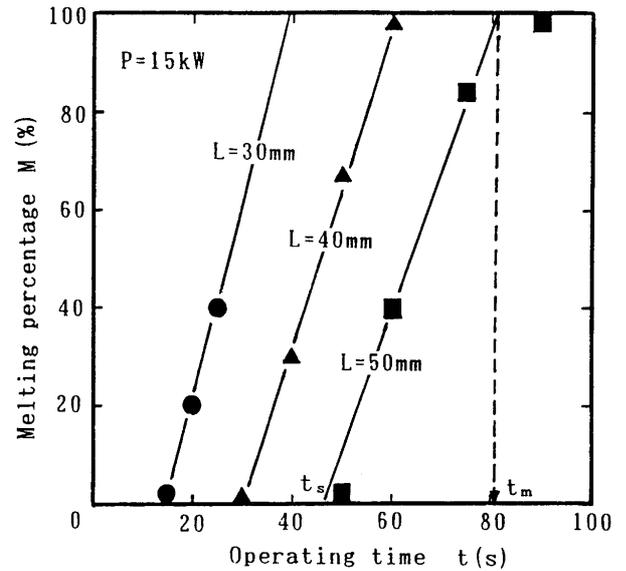The heat transfer of gas tunnel type plasma jet to the copper substrate was measured at each distance from plasma torch (operating distance). **Figure 3** shows the dependence of transferred energy on the distance from torch.

In this case, the power input was $P=15$kW and $P=20$kW respectively. Ar gas flow rate was $Q=200$l/min. The operating distance L was changed from $L=20$mm to $L=80$mm when $P=15$kW.

As shown in these results of both power input, the transferred energy E(kW) was increased expornentially as the distance L was decreased.

In the case of $P=15$kW, the value of transferred enrgy was $E=1.1$kW at the distance of $L=80$mm, while at a short operating distance of $L=20$mm the transferred enrgy was $E=2.1$kW (which was 2 times bigger than that at $L=60$mm).

And for high power input, the heat transfer was increased larger. In the case of $P=20$kW, the value of transferred energy was about $E=2.6$kW at $L=30$mm. This value corresponds to the heat efficiency of about 20% (which shows the ratio against plasma jet energy).

3.3 Melting of aluminum alloy

Figure 4 shows the dependence of melting percentage of aluminum alloy on the operating time of plasma jet. The distance from torch was $L=30$mm, 40mm and 50mm, respectively, when $P=15$kW. The gas flow rate was $Q=200$l/min.

The melting percentage of aluminum alloy M was determined by the ratio of the melting volume V_m to the total volume V. Namely, $M=V_m/V*100$ (%).

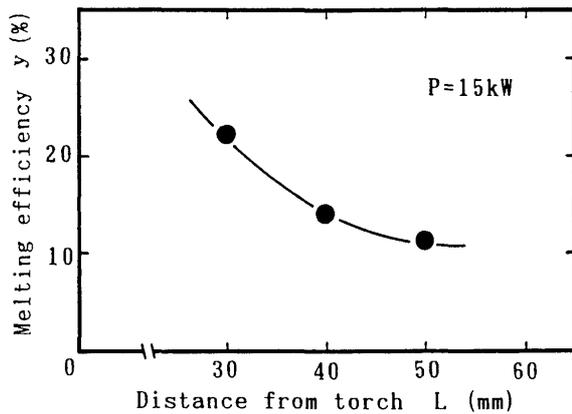The operating time t means the time during which

Fig. 5 Dependence of melting efficiency on distance from torch (melting distance) at $P = 15$kW.

Fig. 6 Dependence of melting time of aluminum on power input at $L = 30$mm.

Fig. 7 Dependence of melting efficiency on power input at $L = 30$mm.

plasma jet is operated to melt the aluminum specimen. The operating time t_s represents the time when the specimen began to melt, and t_m: the time when the specimen was completely melted. At t_m (melting time), the melting percentage M is 100%.

The melting percentage M was linearly increased with the operating time between t_s and t_m. This dependence was a little different at each distance between torch and specimen: at the melting distance of $L = 30$mm the melting time t_m was minimum (t_m was about 39s), and the gradient of melting percentage was sharp. While, at $L = 40$mm and $L = 50$mm , the melting time t_m was larger (t_m was 60s and 81s respectively) and the gradient of M became smaller.

This reason is considered that the longer distance from torch became, the less heat transfer to aluminum specimen was.

Here, we defined melting efficiency y(%), which was the ratio of heat used for melting q against heat input Q in the aluminum alloy, as $y = q/Q*100$. Where $Q = E*t_m$, and $q = (c*T_m + c_m)w$. (w: weight of the specimen, c: specific heat, c_m: heat of fusion). This melting efficiency was obtained by using Fig. 3 and Fig 4.

The dependence of melting efficiency on the distance from torch (melting distance L) at the power input of $P = $ 15kW is shown in **Fig. 5**. As shown in this figure, the melting efficiency y was increased as the melting distance was decreased. And at a shorter distance of $L = 30$mm the melting efficiency was more than 20%.

By means of this plasma melting system, it was found that a lot of thermal energy was lost in an atmosphere from the specimen, and the profile of the melting pot played an important role in order to enhance the melting efficiency.

3.4 Effect of plasma power input on the melting property
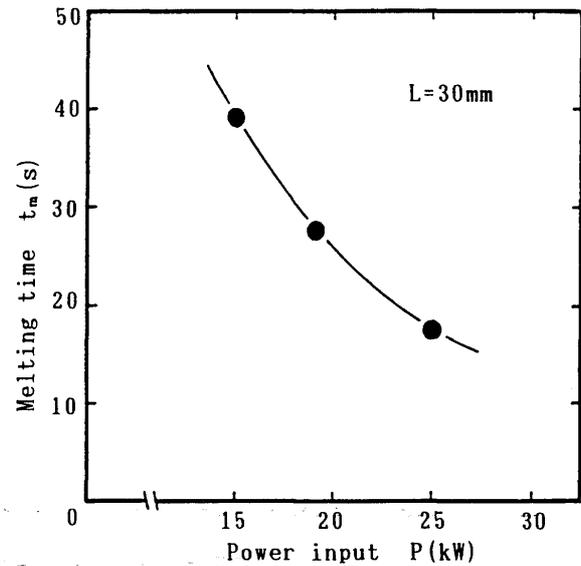
At $L = 30$mm, the power input to torch was changed, and the experiment for melting of aluminum was carried out in the same manner as described above.

Figure 6 shows the dependence of melting time t_m of aluminum specimen on power input P at $L = 30$mm.

It is found that the melting time t_m was decreased expornentially as the power input was increased from $P = 15$kW to $P = 25$kW. This was caused by the fact that the heat input to aluminum (absorbed energy of specimen) was increased greatly with the increase of power input.

The dependence of melting efficiency on the power input at $L = 30$mm is shown in **Fig. 7**. It is found that the melting efficiency y was increased linerly with the increase of the
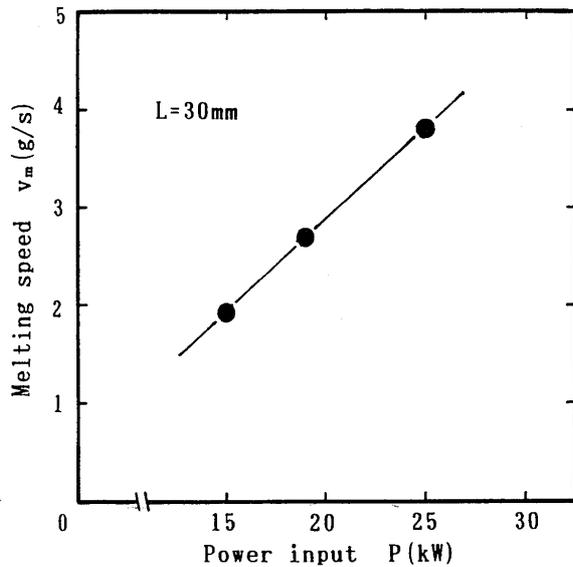
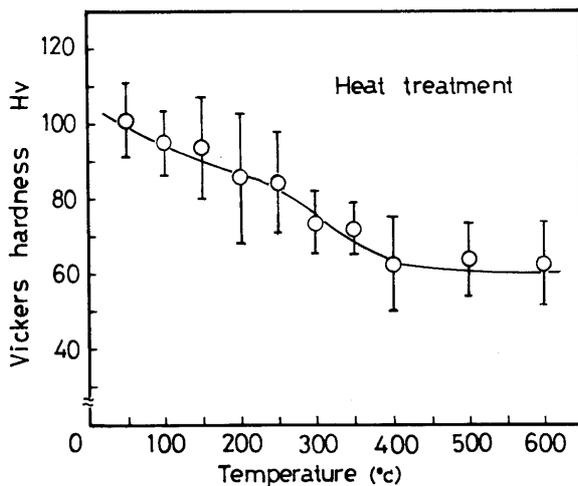Fig. 8 Dependence of melting speed on power input at $L=$ 30mm.

Fig. 9 Dependence of Vickers hardness of the specimen on temperature of heat treatment.

power input P. For $P=25$kW, the melting efficiency was more than $y=30\%$.

This dependence could be explained as follows: the heat transfer to the specimen was much depended upon the melting time as shown in Fig. 6: y is proportional to $(1/t_m)*(1/E)$. As the power input was increased, t_m was decreased largely, so that y was increased like this result, in spite of the increase of E.

The dependence of melting speed of the specimen on the power input is shown in Fig. 8, the melting speed v_m was calculated from the equation of $v_m=w/t_m$ (g/s), where w is weight of specimen and t_m is melting time.

The melting speed was increased linearly with the increase of power input, as well as the case of the melting efficiency as shown in Fig. 7.

3.5　the property of melted aluminum

In this way, the characteristics of plasma melting system have been clarified: a high melting efficiency was obtained at a short melting distance, when the power input P was large.

Then for this melted aluminum, the mechanical property was measured. The Vickers hardness of melted aluminum became lower as compared with that of as received aluminum alloy ($H_V=100-115$). Namely, for melted aluminum, $H_V=60$-70 (average: 65). This value did not depend on the melting condition.

After heat treatment of this aluminum alloy, the Vickers hardness was changed from $H_V=115$ to $H_V=55$ for each temperature of heat treatment as shown in Fig. 9. At high temperature more than 400°C, the values of Vickers hardness were between $H_V=55$ and $H_V=75$. (average: 65).

Thus, after plasma melting, the Vickers hardness became lower than that of as received aluminum alloy, as well as the case of the heat treatment for the temperature more than 400°C.

From the observation of the microstructure of melted aluminum alloy, it was found that the grain size in the structure after plasma melting was changed smaller than that of as recived aluminum alloy (50μm). And it seems that small pores appeared in the grain boundary of melted aluminum alloy.

The result of the measurement of chemical composition showed that the large difference did not exist in the chemical composition of the melted aluminum alloys as compared with that of as received aluminum alloy.

4.　Conclusion

The Al-Mg alloy was melted by using the gas tunnel type plasma jet, and the melting characteristics of this melting system were investigated. The results obtained in this study are summarized as follows.

(1)　According to the calorimetric measurement, the thermal efficiency of gas tunnel type plasma jet was more than 70%. The transferred energy from this plasma jet to the substrate was increased exponentially as the operating distance was decreased.

(2)　Melting characteristics of this system were mainly influenced by the melting conditions such as melting distance, the profile of the melting pot and so on. For example, the melting percentage was increased linearly with the operating time between t_s and t_m. The melting time t_m was increased as the melting distance was

increased. On the other hand, the increase of melting distance caused the decrease of the melting efficiency.

(3) The effect of the power input was very large. Namely, the melting time t_m was decreased as the power input was increased. Therefore the melting speed of the specimen was increased with power input. Melting efficiency became greater when the power input was increased.

(4) After plasma melting, it is found that the Vickers hardness became lower than that of as received aluminum alloy. This value of the Vickers hardness was similar to that of heat treatment at the temperature more than 400°C. The hardness inside the melted specimen was about $H_v = 65$.

Acknowledgement

References

1) Y. Arata and A. Kobayashi: J. A. P., **59**−9 (1986) 1107.

2) Y. Arata and A. Kobayashi: J. J. A. P., **25**−11 (1986) 1697.

3) M. Okada and Y. Arata: "Plasma Engineering", Nikkan Kogyou Shinbun-sha. Tokyo (1965).

4) A. Kobayashi: J. Jpn. Welding Soc. **57**−8 (1988) 307.

5) Y. Arata, A. Kobayashi, Y. Habara and S. Jing: Trans. JWRI. **15**−2 (1986) 227.

6) Y. Arata, A. Kobayashi and Y. Habara: J. High Temp. Soc., **13**−3 (1987) 116 (in Japanese).

7) Y. Arata, Y. Habara and A. Kobayashi: Trans. JWRI, **16**−1 (1987) 31.

8) A. Kobayashi, N. Hasegawa and H. Namikawa: Trans. JWRI, **18**−1 (1989) 13.

9) A. Kobayashi, N. Bessho and M. Higuchi: Trans. JWRI, **19**−2 (1990) 117.